Development 140, 2923-2932 (2013) doi:10.1242/dev.093534

An exclusively mesodermal origin of fin mesenchyme demonstrates that zebrafish trunk neural crest does not generate ectomesenchyme

Raymond Teck Ho Lee[1], Ela W. Knapik[2], Jean Paul Thiery[1,3,4] and Thomas J. Carney[1,*]

SUMMARY

The neural crest is a multipotent stem cell population that arises from the dorsal aspect of the neural tube and generates both non-ectomesenchymal (melanocytes, peripheral neurons and glia) and ectomesenchymal (skeletogenic, odontogenic, cartilaginous and connective tissue) derivatives. In amniotes, only cranial neural crest generates both classes, with trunk neural crest restricted to non-ectomesenchyme. By contrast, it has been suggested that anamniotes might generate derivatives of both classes at all axial levels, with trunk neural crest generating fin osteoblasts, scale mineral-forming cells and connective tissue cells; however, this has not been fully tested. The cause and evolutionary significance of this cranial/trunk dichotomy, and its absence in anamniotes, are debated. Recent experiments have disputed the contribution of fish trunk neural crest to fin osteoblasts and scale mineral-forming cells. This prompted us to test the contribution of anamniote trunk neural crest to fin connective tissue cells. Using genetics-based lineage tracing in zebrafish, we find that these fin mesenchyme cells derive entirely from the mesoderm and that neural crest makes no contribution. Furthermore, contrary to previous suggestions, larval fin mesenchyme cells do not generate the skeletogenic cells of the adult fin, but persist to form fibroblasts associated with adult fin rays. Our data demonstrate that zebrafish trunk neural crest does not generate ectomesenchymal derivatives and challenge long-held ideas about trunk neural crest fate. These findings have important implications for the ontogeny and evolution of the neural crest.

KEY WORDS: Fin mesenchyme, Dermomyotome, Ectomesenchyme, Fibroblast, Neural crest

INTRODUCTION

The neural crest is a multipotent embryonic stem cell population formed during neurulation from which numerous cell types derive, including pigment cells and neurons and glia of the peripheral nervous system (Le Douarin and Kalcheim, 1999). Pioneering histological (Landacre, 1921; Platt, 1893), xenotransplantation (Raven, 1932), quail-chick chimera (Le Lièvre and Le Douarin, 1975), cell labelling (Chibon, 1967; Horstadius and Sellman, 1946; Johnston, 1966) and cell extirpation (Stone, 1926; Stone, 1929) experiments have provided considerable evidence that, in addition to melanocytes and cells of the peripheral nervous system, anterior dorsal neural folds form cranial ectomesenchyme during neurulation. From this population arise skeletogenic, odontogenic and connective tissues of the craniofacial skeleton (reviewed by Le Douarin and Kalcheim, 1999). Despite the long history of neural crest research and the wealth of resulting information, many aspects of neural crest biology remain obscure or contentious. In particular, the precise lineage restriction of neural crest and the extent of its potency are debated.

In amniotes, the cranial neural folds are a major source of cartilage, skeletal and connective tissues of the head, whereas there appears to be no contribution of trunk neural crest to these tissues types of the body. How this dichotomy between trunk and cranial neural crest contributions arose during evolution is unclear. Hypotheses include a trunk environment not permissive for ectomesenchyme (McGonnell and Graham, 2002) and a topologically distinct (and cranial specific) source of ectomesenchyme within the neural ectoderm (Breau et al., 2008; Weston et al., 2004). In fish and amphibia, however, there have been a number of studies proposing that larval fin mesenchyme cells derive from trunk ectomesenchymal neural crest (reviewed by Hall and Hörstadius, 1988; Le Douarin, 1982; Le Douarin and Kalcheim, 1999). This was first suggested in the 1930s based on xenotransplantation and cell staining experiments (Detwiler, 1937; Holtfreter, 1935; Raven, 1936; Raven, 1932). This cell type was assumed to contribute to the connective tissue of the fins and thus to represent an ectomesenchyme derivative. In line with this, we recently described a role for larval fin mesenchyme cells in maturation of fin extracellular matrix (ECM) (Asharani et al., 2012).

The topic was largely neglected for decades until the advent of fluorescent vital dyes permitted cell fate analyses. Fluorescent labelling of *Xenopus* and zebrafish neural tissue supported a contribution of neural crest to larval fin mesenchyme (Collazo et al., 1993; Krotoski et al., 1988; Smith et al., 1994). However, in many of these experiments it was noted that tissue labelling was not always precise, and definitive characterisation of the derivative cells was not possible. Indeed, further vital dye labelling experiments identified an additional mesodermal contribution to fin mesenchyme cells of both the ventral (Tucker and Slack, 2004) and dorsal (Garriock and Krieg, 2007) larval fins, which has been confirmed by transplantation experiments in axolotls (Sobkow et al., 2006). Crucially, the relative contribution of the neural crest and mesoderm to fin mesenchyme cells has never been determined.

[1]Institute of Molecular and Cell Biology (IMCB), A*STAR (Agency for Science, Technology and Research), 61 Biopolis Drive, Singapore 138673, Singapore. [2]Department of Medicine, Division of Genetic Medicine, Vanderbilt University Medical Center, Nashville, TN 37232, USA. [3]Department of Biochemistry, Yong Loo Lin School of Medicine, National University of Singapore, 117597, Singapore. [4]Cancer Science Institute, National University of Singapore, 117599, Singapore.

*Author for correspondence (tcarney@imcb.a-star.edu.sg)

Accepted 29 April 2013

In addition to larval fin mesenchyme cells, trunk neural crest of teleosts had also been assumed to generate other ectomesenchymal derivatives, namely components of the adult post-cranial exoskeleton, which include the bony fin rays (lepidotrichia) and scales (Sire and Akimenko, 2004; Smith et al., 1994; Smith and Hall, 1990). Such assumptions were based on the fact that some integumentary skeletal elements were believed to comprise odontogenic tissues and/or dermal bone. In mammals, these tissue types were long assumed to be generated exclusively by the cranial ectomesenchymal neural crest. For example, in evolutionary terms, the first mineralised tissue to arise in vertebrates is considered to be the mineralised body armour and teeth of stem gnathostomes [specifically conodont teeth; although conodont classification as stem gnathostomes and even vertebrates is contested (Donoghue et al., 2000; Turner et al., 2010)]. The fact that mineralised body armour was formed from dentine, a tissue unique to neural crest, led to speculation that the post-cranial odontogenic skeletal elements of early vertebrates were generated from trunk neural crest (Sire et al., 2009). The identification of a latent skeleto/odontogenic potential of chick and mouse trunk neural crest cells, as revealed upon culturing in appropriate artificial conditions, was supportive of this scenario, as was the identification of trunk ectomesenchyme in extant fish and amphibia (Abzhanov et al., 2003; Lumsden, 1988; McGonnell and Graham, 2002). Evidence for the existence of trunk ectomesenchyme thus has important implications for understanding the evolution of skeletogenesis. However, more recent identification of an additional mesodermal contribution to the dermal bones of the cranial vault (reviewed by Gross and Hanken, 2008) suggested that dermal bones of the fins might not necessarily derive exclusively from neural crest. We have recently provided the first test of a neural crest origin of post-cranial dermal bone and scales in fish, and found that fin osteoblasts and scale mineral-forming cells, previously considered to be a trunk ectomesenchymal neural crest derivative, are in fact generated by paraxial mesoderm, with no discernible contribution from neural crest (Lee et al., 2013) (see also Mongera and Nüsslein-Volhard, 2013; Shimada et al., 2013). This surprising result led us to question the extent to which trunk neural crest generates larval fin mesenchyme, the only other described ectomesenchymal neural crest derivative of the trunk.

Through marker analysis, genetic ablation, transgenic labelling and time-lapse approaches we demonstrate that, as with fin osteoblasts, the mesenchyme of both the dorsal and ventral larval fins derives almost exclusively from the dermomyotome compartment of the paraxial mesoderm, whereas neural crest does not contribute. Further, we show that larval fin mesenchyme cells are retained into the adult fin where they become fin fibroblasts. Our data demonstrate that the trunk neural crest of zebrafish does not contribute any ectomesenchymal derivatives and suggest that anamniotic trunk neural crest possesses the same diversity of fates as the trunk neural crest of amniotes.

MATERIALS AND METHODS

Fish husbandry and lines

Fish were maintained in the IMCB zebrafish facility and embryos were obtained through natural crosses and staged according to Kimmel et al. (Kimmel et al., 1995). *mos*$^{-/-}$*; mob*$^{-/-}$ larvae were generated as described (Wang et al., 2011); the generation of the ET37 and ET5 lines is outlined by Parinov et al. (Parinov et al., 2004). For lineage analyses we used the previously described transgenic lines *Tg(UAS:Kaede)*^{rk8} (Hatta et al., 2006), the *ubi:switch* Cre recombination reporter line *Tg(−3.5ubb:loxP-EGFP-loxP-mCherry)*^{cz1701} (Mosimann et al., 2011), the α-actin Gal4 line *Tg(actc1b:Gal4)*^{i269} (Maurya et al., 2011), the Sox10 eGFP line *Tg(−4.9sox10:eGFP)*^{ba2} (Carney et al., 2006) and the Pax3a eGFP line *TgBAC(pax3a:EGFP)*^{i150} (Seger et al., 2011).

In situ hybridisation and immunostaining

Whole-mount embryo RNA *in situ* hybridisation was performed as described (Thisse and Thisse, 2008), developed with NBT/BCIP (Roche) and cleared in glycerol prior to imaging. Probes used were *bmp1a* (Asharani et al., 2012), *hmcn2* (Carney et al., 2010) and *fbln1* (Feitosa et al., 2012). Whole-mount embryo fluorescent immunostaining was performed as described (Asharani et al., 2012). Primary antibodies were: rat anti-eGFP (1:250; 04404-26, Nacalai Tesque), chicken anti-eGFP (1:500; ab13970, Abcam), rabbit anti-Kaede (1:250; PM012, MBL International), rabbit anti-DsRed/mCherry (1:250; 632496, BD Biosciences), mouse anti-Pax3/7 [1:200; DP312 (Davis et al., 2001)] and mouse zns-5 (1:200; Zebrafish International Resource Center). Primary antibodies were detected using fluorescently conjugated secondary antibodies (1:400). Secondary antibodies were raised in donkey and were purchased from Jackson ImmunoResearch (Dylight 488 anti-chicken, Dylight 649 anti-rat) or Invitrogen (Alexa 546 anti-rabbit, Alexa 488 anti-rabbit, Alexa 647 anti-mouse, Alexa 546 anti-mouse).

Sectioning, microscopy and photoconversion

For transverse sections, embryo steaks were cut after *in situ* hybridisation or immunostaining using scalpel blades. Alternatively, cryosectioning was performed on embryos or adult fins using a Leica CM1900 cryostat, and the 16 μm sections then fluorescently immunostained. Confocal images and time-lapse movies were taken on an inverted Zeiss LSM700 or an upright Olympus BX61 Fluoview microscope, and high-magnification brightfield or Nomarski images were taken on a Zeiss AxioImager M2. For low-magnification brightfield images a Leica MZ16F stereoscope was used. For time-lapse recordings of caudal fin development, anaesthetised embryos were mounted in 1% low melting point agarose (MO BIO Laboratories) in glass-bottom imaging dishes (MatTek) supplemented with 0.02% tricaine (buffered to pH 7.0). Once solidified, the agarose was excavated from around the tail of the embryos to permit normal tail morphogenesis, and the embryo overlaid with 0.5× E2 medium (7.5 mM NaCl, 0.25 mM KCl, 0.5 mM $MgSO_4$, 75 μM KH_2PO_4, 25 μM Na_2HPO_4, 0.5 mM $CaCl_2$, 0.35 mM $NaHCO_3$) containing 0.02% buffered tricaine.

To follow Kaede-expressing cells by photoconversion, 24-hpf Kaede-positive embryos were mounted in agarose and imaged by confocal microscopy. A selected region of interest was converted using 60-80 pulses of 405 nm wavelength UV laser illumination. Embryos were then re-imaged immediately before being rescued from the agarose, and then re-examined 1 day later at 48 hpf.

Tamoxifen treatment

To induce Cre activity at specific time points in *Cre*^{ERt2} transgenic embryos, 4-hydroxytamoxifen (Sigma) was dissolved in ethanol and added to dechorionated embryos in embryo medium at a final concentration of 5 μM as described (Mosimann et al., 2011). After exposure, the embryo medium was replaced and embryos were allowed to develop and then assessed for mCherry expression.

PCR, transgene construct cloning, BAC recombineering and RNA synthesis

PCR amplification was performed using PrimeStar (Takara Bio) on a DNA Engine thermocycler (BioRad). A 2.1 kb promoter region of *ntla* was amplified by PCR from genomic DNA and cloned into the p5E-MCS vector (Kwan et al., 2007) by restriction digestion and ligation to generate p5E-2.1*ntla*. The 7.2 kb *sox10* promoter (Dutton et al., 2008) and the 1.7 kb *tbx6* promoter (Szeto and Kimelman, 2004) were transferred from standard vectors to p5E-MCS by restriction digestion and ligation. All transgene constructs were generated using multisite Gateway cloning methodology through the zebrafish Tol2kit (Kwan et al., 2007). Middle entry vectors containing lyn-tdTomato, Gal4VP16, Cre and Cre^{ERt2} were used in LR Clonase II Plus (Invitrogen) based recombination reactions. Reactions were conducted with Tol2-containing destination vectors, with or without the *cmlc2:egfp* transgenesis marker where required.

The *hmcn2:Cre*^{ERt2} BAC was generated by recombining a *Cre*^{ERt2} cassette flanked by 60 bp arms homologous to the region around the translation start of the *hmcn2* gene. Recombination was performed using

RedET methodology (GeneBridges). A second recombination was performed targeting a Tol2-containing cassette (Suster et al., 2009) to the BAC vector, thus allowing improved efficiency of transgenesis.

Tol2 RNA was synthesised from *Sma*I-linearised plasmid template and transcription performed with T3 RNA polymerase (Ambion).

Embryo injection and transgenesis

Plasmid DNA was prepared using the HiSpeed Plasmid Midi Kit (Qiagen) and BAC DNA using NucleoBond BAC 100 (Machery-Nagel). Embryos were injected with 30 ng/µl plasmid DNA and 30 ng/µl *Tol2* RNA diluted in Phenol Red and Danieau's buffer using a PLI-100 microinjector (Harvard Apparatus).

RESULTS

Substantial mesodermal contribution to larval fin mesenchyme

We have recently identified that *in situ* probes detecting *bmp1a* (Asharani et al., 2012), *hemicentin 2* (*hmcn2*) (Carney et al., 2010) and *fibulin 1* (*fbln1*) (Feitosa et al., 2012) mark fin mesenchyme cells from 48 hpf onwards (Fig. 1G,J,M). In addition, these cells are labelled by the enhancer trap lines ET37 and ET5 (Parinov et al., 2004), which also express eGFP in the apical ridge of the fins (Fig. 1A,D). Preceding this fin mesenchyme expression, all these markers shared a somitic expression domain, rather than neural crest expression, although ET5 was somewhat broader (Fig. 1B,C,E,F,H,I,K,L,N,O). This was surprising given the previous reports of at least a partial neural crest contribution to fin mesenchyme, and led us to investigate the source of these cells.

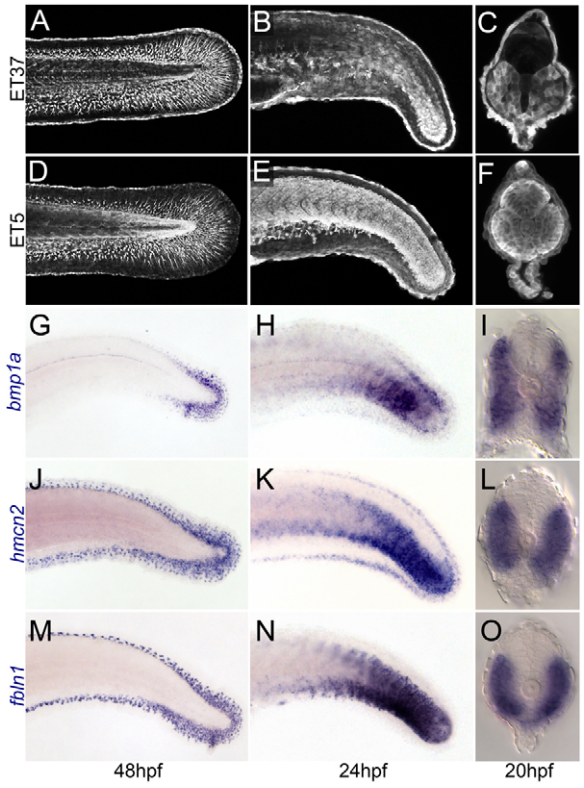

Fig. 1. Paraxial mesoderm expression often precedes fin mesenchyme expression. (**A-F**) Confocal images of the trunk and tail regions of the ET37 (A-C) and ET5 (D-F) zebrafish lines immunofluorescently stained for eGFP. Lateral views at 48 hpf (A,D) and 24 hpf (B,E) show that expression in fin mesenchyme follows earlier expression in the mesoderm. Transverse confocal images of the trunk of ET37 (C) and ET5 (F) at 20 hpf show expression in paraxial mesoderm as well as at other sites. (**G-O**) Micrographs of embryos stained by *in situ* hybridisation with probes against *bmp1a* (G-I), *hmcn2* (J-L) and *fbln1* (M-O). Lateral views show the fin mesenchyme expression at 48 hpf (G,J,M) and the preceding mesodermal expression at 24 hpf (H,K,N). Mesodermal expression is paraxial as shown in images of transverse sections of 20-hpf embryos viewed with Nomarski optics (I,L,O).

Expression domains can be dynamic, and it is possible that the somitic expression is not temporally contiguous with fin mesenchyme expression. To test this, we used time-lapse microscopy of the ET37 line to visualise the source of fin mesenchyme cells and noted that expression of eGFP was not biphasic, but continuous from the somitic expression through to fin mesenchyme cells (supplementary material Movies 1 and 2). We were able to track individual cells emigrating from both the ventral (Fig. 2A; supplementary material Movie 1) and dorsal (Fig. 2B; supplementary material Movie 2) somites into the fins where they became fin mesenchyme cells. To confirm that we were not tracking ectopically labelled neural crest cells, we generated a transgenic line that labels mesoderm with lyn-tdTomato using the *ntla* promoter (*ntla:lyn-tdtomato*) (Harvey et al., 2010). At 24 hpf in the ventral fin, tdTomato-positive cells could be seen as epithelial cells within somitic regions (Fig. 2C, left panel), a location and morphology inconsistent with neural crest cells. Time-lapse analysis of this line in the ET37 background confirmed that the eGFP-positive fin mesenchyme cells were derived from these *ntla*-expressing epithelial mesodermal cells (Fig. 2C; supplementary material Movie 3).

To determine whether the contribution of the mesoderm was more extensive, we generated two lines expressing Gal4 in paraxial mesoderm using either the *ntla* promoter or the *tbx6* promoter (Szeto and Kimelman, 2004), and crossed them to the *uas:kaede*^{rk8} transgenic line (Hatta et al., 2006). In both lines, we noted strong paraxial mesodermal Kaede fluorescence at 24 hpf (Fig. 3A,D; data not shown), with the *tbx6* promoter exhibiting a slightly more restricted expression pattern. Kaede protein was then photoconverted by UV laser at 24 hpf in either broad ventral or dorsal regions of the tail mesoderm (Fig. 3B,B′,E,E′). Imaging these embryos the following day revealed extensive labelling of mesodermal derivatives within the converted region, including muscle fibres as well as a large number of mesenchyme cells in the adjacent fin (Fig. 3C,C′,F,F′). This is consistent with our time-lapse data in demonstrating that fin mesenchyme derives from directly adjacent somitic domains.

Neural crest does not generate fin mesenchyme

Our data demonstrate that in zebrafish at least a significant proportion of both the dorsal and ventral fin mesenchyme cells are derived from the mesoderm. Recent literature has suggested that in amphibia the fin mesenchyme cells have a dual origin, deriving from both mesoderm and neural crest (Garriock and Krieg, 2007; Sobkow et al., 2006; Tucker and Slack, 2004). We quantified the extent of neural crest contribution to fin mesenchyme cells, again exploiting the stability of Kaede in zebrafish as a lineage label (Dixon et al., 2012). We used the *sox10* premigratory neural crest promoter (Carney et al., 2006) to generate a *sox10*:*gal4* transgenic line and crossed it to *uas:kaede* transgenic fish. Double-transgenic offspring showed extensive labelling of neural crest derivatives at 48 hpf in the trunk, including pigment cells, cells in the branchial arches and associated with the forming dorsal root ganglia (Fig. 4A-A″; supplementary material Fig. S1).

To quantify the extent of neural crest labelling, we counted the number of Kaede-positive melanophores at 30 hpf, and noted that

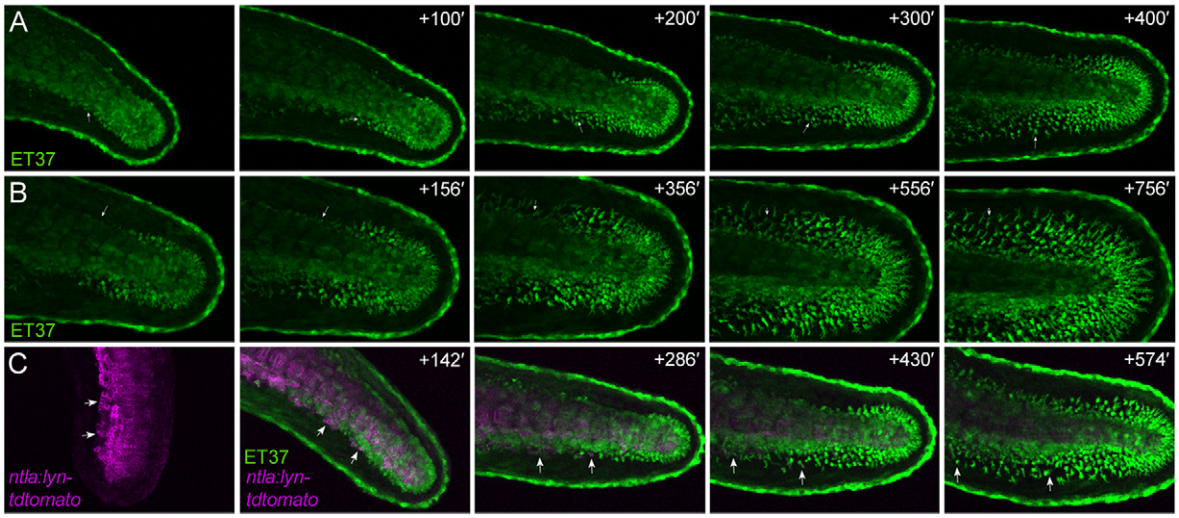

Fig. 2. Fin mesenchyme cells emerge from trunk mesoderm. Stills of time-lapse Movies 1-3 (see supplementary material Movies 1-3) of the tail of the ET37 line alone (**A**,**B**) or crossed to the *ntla:lyn-tdtomato* transgenic line (**C**). eGFP is shown in green and membrane-tdTomato is in magenta. Left panels are taken at ~26 hpf (A), 29 hpf (B) and 22 hpf (C), with subsequent time points (indicated in minutes) shown in panels to the right. Examples of fin mesenchyme cells are indicated (arrows) emerging from the ventral (A,C) and dorsal (B) mesoderm into the adjacent fin. First panel of C is shown without eGFP signal to highlight the epithelial nature of the cells within the mesoderm prior to fin immigration.

at least 93% (507/545 in five embryos) of melanophores examined were Kaede positive. We observed a limited number of Kaede-positive cells in the posterior fin (Fig. 4B,B′); however, crossing these double transgenics onto the ET37 background and immunostaining for eGFP and Kaede demonstrated that Kaede-positive neural crest cells never co-expressed eGFP (0/12 embryos analysed; Fig. 4C-C″), and thus cells of the fins that were derived from *sox10*-expressing neural crest do not appear to be fin mesenchyme cells. Indeed, upon imaging these cells under transmitted or incident light, we noted that in most cases the Kaede-positive cells displayed clear characteristics of pigment cells, either black melanophores (supplementary material Fig. S2A-B″), blue/yellowish xanthophores (supplementary material Fig. S2B-C″) or iridescent iridophores (supplementary material Fig. S2C-C″). Occasionally Kaede-positive cells were seen in the fin that had no discernible pigmentation yet had a morphology inconsistent with fin mesenchyme and were never eGFP positive in the ET37 line. The identity of these cells is unknown but they might represent immature pigment cells. We conclude that, although neural crest cells do invade the zebrafish fin, they mostly generate pigment cells and do not appear to contribute to fin mesenchyme.

As an independent confirmation of our Kaede result, we generated a transgenic line expressing Cre recombinase under the *sox10* promoter and crossed this to the *ubi:switch* reporter line (Mosimann et al., 2011), thus permanently labelling *sox10*-expressing cells with mCherry. The neural crest is labelled robustly and broadly at all axial levels (Lee et al., 2013). Imaging these embryos at 72 hpf demonstrated again that, whereas neural crest derivatives were mCherry positive, there were no mCherry-positive fin mesenchyme cells (supplementary material Fig. S3A,A′).

We complemented these cell labelling data with an analysis of zebrafish embryos in which the neural crest had been genetically ablated. Zebrafish embryos doubly deficient for both *tfap2a* (*mont blanc*, *mob*^{m610}) and *foxd3* (*mother superior*, *mos*^{m188}) (*mob;mos* embryos) have been shown to lack neural crest induction and are devoid of almost all neural crest derivatives (Wang et al., 2011) (Fig. 4D,E). If there is a neural crest contribution to fin mesenchyme, we might expect a reduction in the number of fin mesenchyme cells in *mob;mos* embryos. These embryos fully retained their medial fins, within which statistically indistinguishable numbers of fin mesenchyme cells were observed in both the wild-type and *mos;mob* embryos (Fig. 4F-H). It remains possible that loss of neural crest-derived fin mesenchyme could be obscured in this experiment through compensation from the mesoderm. However, in light of the genetic labelling experiments described above, we interpret the lack of any measurable fin mesenchyme reduction upon neural crest ablation as indicating no, or extremely limited, neural crest contribution.

Paraxial mesoderm is the source of all fin mesenchyme

We have provided evidence that both dorsal and ventral fin mesenchyme derives, at least partially, from paraxial mesoderm and not from neural crest. We next sought to determine whether the mesodermal contribution could account for all fin mesenchyme cells. We noted during our analysis of the *tbx6:gal4; uas:kaede* and the *ntla:gal4; uas:kaede* embryos there was strong perdurance of Kaede protein to 48 hpf within fin mesenchyme and that in both lines the majority of fin mesenchyme cells were Kaede positive (Fig. 5A; data not shown). Neither migratory neural crest nor its derivatives were labelled by Kaede at 24 hpf (supplementary material Fig. S4A-A″) or 48 hpf (data not shown). Crossing the *ntla:gal4; uas:kaede* line to ET37 demonstrated that all fin mesenchyme cells labelled by eGFP are also Kaede positive (Fig. 5B-B″). This co-expression could be due to *de novo* expression from the *ntla* promoter within the fin mesenchyme cells at 48 hpf or represent perdurance from earlier promoter activity within the mesoderm. The former is unlikely as *in situ* hybridisation fails to detect *ntla* transcripts in fin mesenchyme cells at 48 hpf (data not shown) and our time-lapse analysis of the *ntla:lyn-tdtomato* transgenics (Fig. 1C; supplementary material Movie 3) revealed rapid and permanent loss of tdTomato fluorescence in fin mesenchyme cells after immigration into the fin. To demonstrate

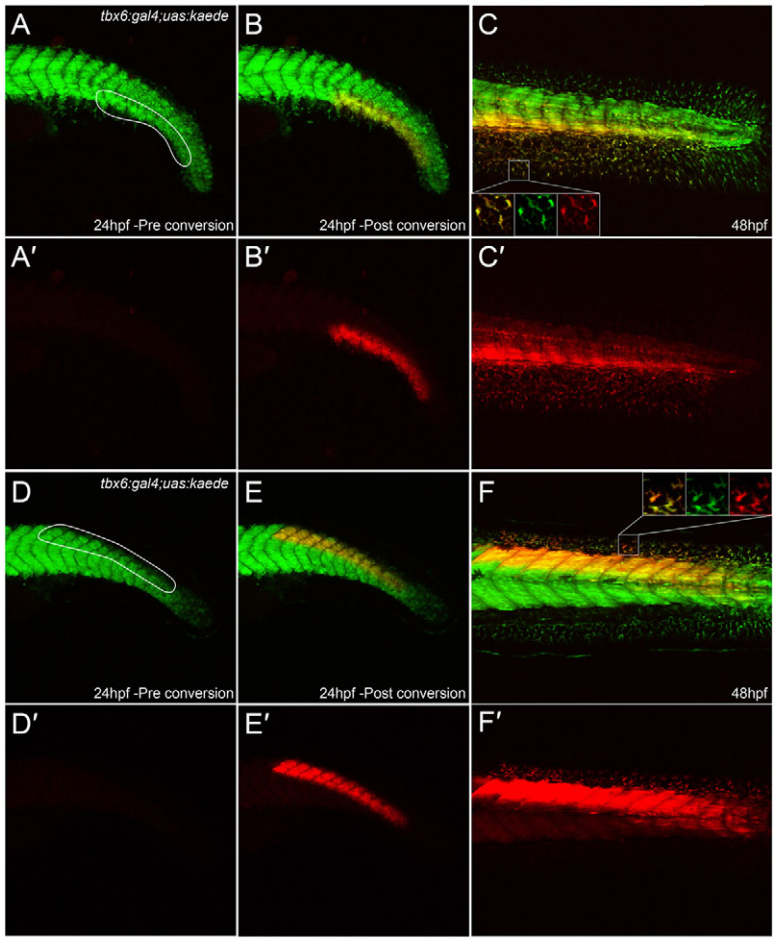

Fig. 3. Extensive contribution of mesoderm to fin mesenchyme. (**A-F′**) Tail of *tbx6:gal4; uas:kaede* embryos at 24 hpf (A-B′,D-E′) and 48 hpf (C,C′,F,F′) both prior to (A,A′,D,D′) and after (B-C′,E-F′) Kaede photoconversion. Unconverted Kaede protein is in green, overlaid with UV-photoconverted Kaede in red (A-F); the red channel is additionally displayed alone for clarity (A′-F′). Ventral (A-C′) and dorsal (D-F′) regions converted by UV laser are outlined in A and D. At 48 hpf, converted cells can be seen in the adjacent fins (magnified in insets in each channel and merged, C,F) and muscle blocks (C,C′,F,F′).

that the expression in the fin mesenchyme represents perdurance from earlier mesodermal expression, we photoconverted the Kaede in the tail of *ntla:gal4; uas:kaede* transgenics at 24 hpf (supplementary material Fig. S5A-B′). Twenty-four hours later we observed almost complete expression of converted Kaede in the fin mesenchyme (supplementary material Fig. S5C,C′), demonstrating that the expression of Kaede in fin mesenchyme derives from the earlier somitic expression.

In addition, we used the Cre-Lox system as an independent lineage labelling method to confirm this result. *tbx6:Cre; ubi:switch* double-transgenic embryos showed induction of mCherry within the *tbx6* expression domain and, later, broad mCherry expression within the fin mesenchyme domain (supplementary material Fig. S3B,B′). Thus, using two independent cell lineage tracing systems driven by two different promoters, we have demonstrated that fin mesenchyme cells are generated entirely from mesoderm and are not neural crest derived.

Fin mesenchyme is a dermomyotome derivative

To delineate the somitic compartment from which fin mesenchyme is derived, we labelled the myotome using the α-actin transgenic line *Tg(actc1b:Gal4^{i269})* (Maurya et al., 2011) and the sclerotome with a transgenic line, *Tg(Ola-Twist:Gal4)*, in which the medaka *Twist* promoter (Inohaya et al., 2007) drives Gal4. Crossing both of these to the *uas:kaede* line allowed us to trace derivatives of the myotome and sclerotome. Despite observing cells in the expected locations at 24 hpf and 48 hpf (supplementary material Fig. S4B-B″; data not shown), we did not observe Kaede fluorescence in the fin mesenchyme in either case (Fig. 5C-D′). Lack of myotome or sclerotome contribution to fin mesenchyme indicated they were likely to be derived from the dermomyotome compartment. Indeed, when we analysed the *TgBAC(pax3a:eGFP)* transgenic line (Seger et al., 2011), which reproduces the expression of Pax3 in the dermomyotome (see also supplementary material Fig. S4C-C″), we noted expression of eGFP in almost all fin mesenchyme cells at 48 hpf (Fig. 5E,E′). To confirm that this is not *de novo* expression in the fin mesenchyme and represents perdurance of eGFP from the dermomyotome at 24 hpf, we performed time-lapse microscopy and observed eGFP-positive fin mesenchyme cells emerging from the somites and invading the fin (two dermomyotome cells are tracked in Fig. 5F; supplementary material Movie 4). Additionally, the neural crest is strongly labelled in this line. Although neural crest cells also invaded the fins they were clearly discernible from fin mesenchyme cells based on their size, eGFP intensity and migratory behaviour.

We conclude that fin mesenchyme cells are dermomyotome derivatives and that, coupled with their morphology, expression of ECM molecules and modifying enzymes as well as a described role in ECM remodelling, they can be considered fibroblasts.

Fin mesenchyme cells persist in the fins into adulthood as fibroblasts

We have recently shown that lepidotrichial skeletogenic cells invade the adult fin between 2 and 3 weeks of age, and do not arise from cells present in the larval fin fold at 5 dpf (Lee et al., 2013). If fin mesenchyme cells do not generate the osteoblasts of the fin

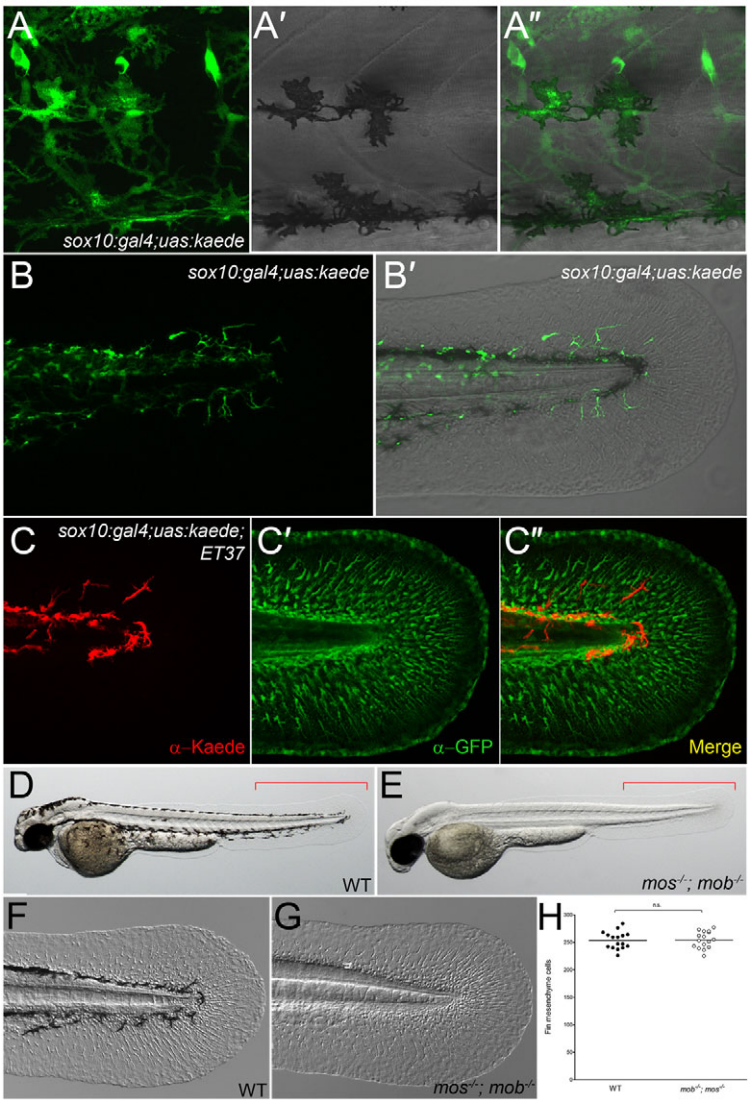

Fig. 4. Neural crest cells do not contribute to fin mesenchyme. (**A-B′**) Lateral trunk (A-A″) and tail region (B,B′) of 48-hpf *sox10:gal4; uas:kaede* transgenic embryos. Kaede protein fluorescence (green) is observed in melanophores (A-A″), nascent dorsal root ganglia and spinal nerves (A), as well as in the fin (B,B′). (**C-C″**) Immunofluorescent labelling of Kaede (red, C), eGFP (green, C′) and merged image (C″) of the fin of a *sox10:gal4; uas:kaede*; *ET37* transgenic embryo. (**D-G**) Overviews (D,E) and Nomarski images (F,G) of 48-hpf wild-type (WT) (D,F) and $mos^{-/-}; mob^{-/-}$ (E,G) embryos showing loss of pigment but presence of a fully formed medial fin (E) with fin mesenchyme cells (G) in the double mutant. Red brackets indicate the region used for quantifying fin mesenchyme cells in H. (**H**) Quantification of fin mesenchyme cells in 12 WT and 12 $mos^{-/-}; mob^{-/-}$ embryos at 48 hpf. No significant differences (n.s.) were observed (two-tailed Student's *t*-test). Bars indicate the mean.

rays, we questioned whether they contribute to any of the cells of the adult fin or are lost during juvenile stages of development. To address this, we conducted time point analysis of *tbx6:Cre^{ERt2}; ubi:switch* transgenics. Embryos were treated with 4-hydroxytamoxifen from 8 hpf to 48 hpf to label cells of the paraxial mesoderm. As with the *tbx6:Cre; ubi:switch* double transgenics, we observed fin mesenchyme cells in the fins of a number of individuals at 5 dpf (Fig. 6A). We followed these cells over subsequent days and noted that they remained within the fin until at least 21 dpf, when chains of cells were also observed (Fig. 6B).

To assess whether they persist into adult stages, we permanently and specifically labelled them by generating an *hmcn2:Cre^{ERt2}* transgene through BAC homologous recombination (see Materials and methods). This construct was injected into the *ubi:switch* transgenic line and subsequently treated with 4-hydroxytamoxifen at 80-116 hpf. Three days later at 7 dpf, scattered mCherry-positive fin mesenchyme cells could be seen within the fin (Fig. 6C). At 3 months of age, these embryos showed extensive labelling of fibroblast-like cells both within the fin rays and in the inter-ray region, but no labelling of osteoblasts (as detected with zns-5 antibody) (Fig. 6D,E). Thus, we confirmed that fin mesenchyme cells do not later generate osteoblasts of the fin rays but persist into the adult fin ray as fibroblasts.

DISCUSSION

The emergence of neural crest was a pivotal moment in the evolution of vertebrates and has been proposed to have occurred at the anterior of a hypothetical protochordate during the generation of a 'new head' (Gans and Northcutt, 1983). Here, neural crest was proposed to take on many roles of the trunk mesoderm, generating head connective and skeletal tissues (ectomesenchyme). There has been considerable conjecture as to whether trunk neural crest also evolved to generate such ectomesenchymal derivatives. Evidence of a neural crest contribution to fin connective tissue in amphibia has been invoked as evidence in support of this. Indeed, we have demonstrated that fin mesenchyme does resemble and function as fibroblastic connective tissue cells. However, through transgenic cell lineage tracing and mutant analysis, we have shown that zebrafish fin mesenchyme is not a derivative of trunk neural crest but is entirely derived from paraxial mesoderm, specifically the dermomyotome. This, in combination with our previous result that mineralising cells of the adult fin rays and scales are not an ectomesenchymal

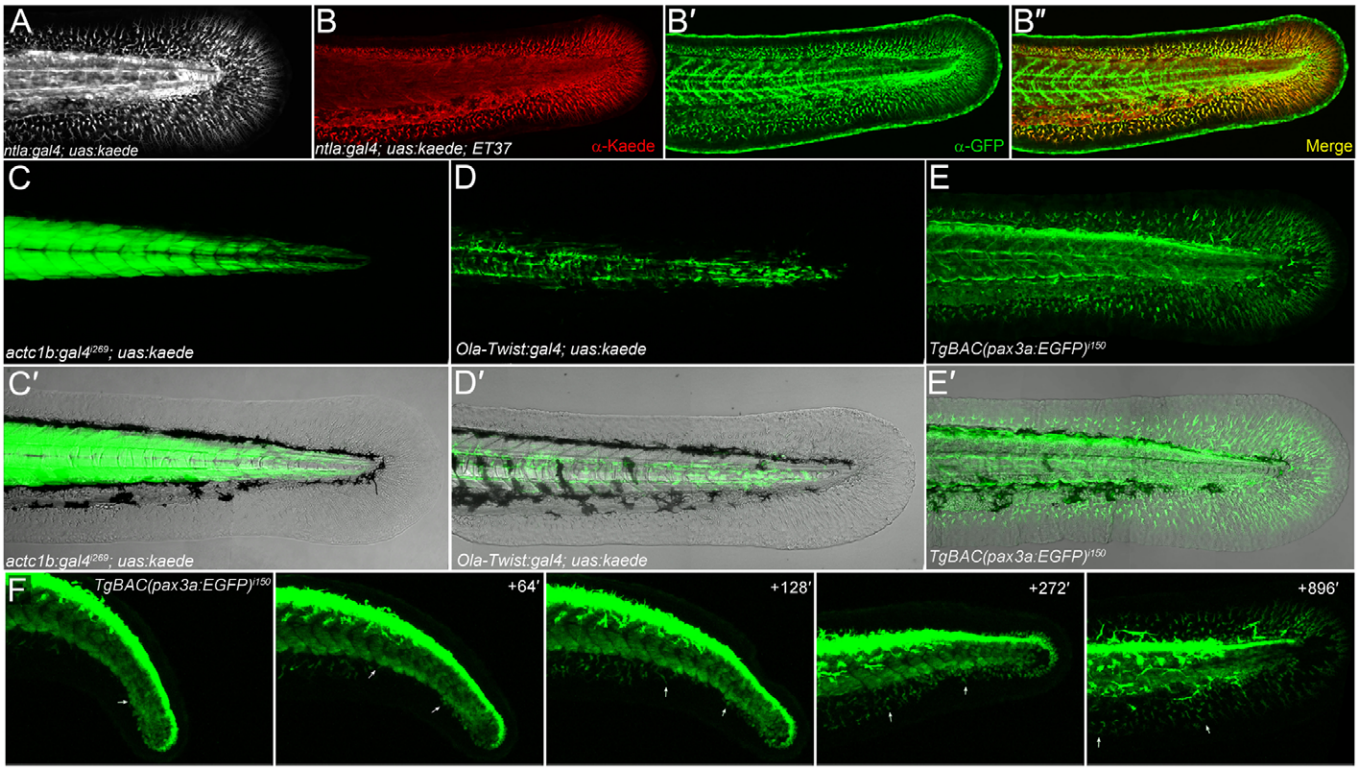

Fig. 5. All fin mesenchyme cells derive from paraxial mesoderm. (**A**) Confocal image of the tail region of a 48-hpf *ntla:gal4; uas:kaede* embryo. (**B-B″**) Immunofluorescent staining of 48-hpf *ntla:gal4; uas:kaede*; *ET37* triple transgenic embryo showing total overlap (B″) of Kaede signal (red, B,B″) and eGFP (green, B′,B″) in the fin. (**C-E′**) Fluorescent images alone (C,D,E) and superimposed on Nomarski images (C′,D′,E′) of the trunk/tail of 48-hpf embryos. The myotome (C,C′), sclerotome (D,D′) and dermomyotome (E,E′) are labelled by *actc1b:Gal4[i269]; uas:kaede* (C,C′), *Ola-Twist:Gal4; uas:kaede* (D,D′) and *TgBAC(pax3a:EGFP)[i150]* (E,E′) transgenics, respectively. (**F**) Stills taken from time-lapse Movie 4 (see supplementary material Movie 4) of the tail region of a *TgBAC(pax3a:EGFP)[i150]* embryo at 24 hpf (left panel) with subsequent time points at given intervals (in minutes) in the panels to the right. Two fin mesenchyme cells can be tracked (arrows) from the dermomyotome into the fins. Note that eGFP expression is higher in neural crest and dorsal neural tube than in dermomyotome.

neural crest derivative (Lee et al., 2013), suggests that the trunk neural crest of zebrafish does not have ectomesenchymal fates, and thus resembles mammalian trunk neural crest in its repertoire of derivatives. This challenges long-held ideas about trunk neural crest lineages in anamniotes.

It should be noted that previous work has led to the belief that trunk neural crest in amphibia partially contributes (along with mesoderm) to fin mesenchyme. A single cell type originating from two distinct germ layers in a simple tissue such as the fin fold seems unusual, although a mixed origin is observed in more complex anatomical structures such as the calvaria (Gross and Hanken, 2008). While it is possible that the trunk neural crest of amphibia is unique in this regard and has acquired ectomesenchyme fates during evolution (or, conversely, mammals and teleosts have independently lost this lineage from trunk neural crest), in light of our data it would be worthwhile re-examining the fates of amphibian trunk neural crest more precisely. Our analysis indeed demonstrated the extremely close proximity of neural crest and dermomyotome during early development as well as a neural crest contribution of pigment cells to the fin. These might have complicated compartment labelling and derivative identification in previous analyses. We were also surprised to find during our mutant analysis that in embryos in which neural crest was not induced we still observed a fully formed fin fold. It has been shown in amphibia that neural crest is necessary for fin fold induction in larvae; however, these experiments were based on surgical ablation (DuShane, 1935; Tucker and Slack, 2004). The ability of the *mos;mob* mutants to induce fin fold suggests that this process does not require differentiated neural crest. It is possible that this fin-inducing signal emanates from cells within the neural crest territory of the neural plate but does not require induction of neural crest. It will be informative to determine the identity, origin and timing of this inducing signal from the neural plate.

One implication of our findings concerns the existence and properties of neural crest cells *in vivo*. An extensive body of evidence has shown that pigment cells, peripheral neurons and glia share a common precursor with ectomesenchymal derivatives within cranial neural folds (Baroffio et al., 1991; Blentic et al., 2008; Chan and Tam, 1988; Essex et al., 1993; Osumi-Yamashita et al., 1994; Pohl and Knöchel, 2001). More recent experiments in the mouse mapped the cranial neural fold territory with greater spatial and temporal resolution, and led to the controversial proposal of a distinct origin (the metablast) for ectomesenchyme (Breau et al., 2008; Weston et al., 2004). Although this contentious notion is less well accepted, such a topological partitioning of ectomesenchyme and non-ectomesenchyme birth sites would be incompatible with the model of a homogeneous multipotent neural crest territory. In agreement with this segregation model was the observation that neural crest cells are fate restricted in the zebrafish head and trunk prior to delamination (Raible and Eisen, 1994; Schilling and Kimmel, 1994). Although our investigations do not address the question of the existence of a metablast directly, they do argue

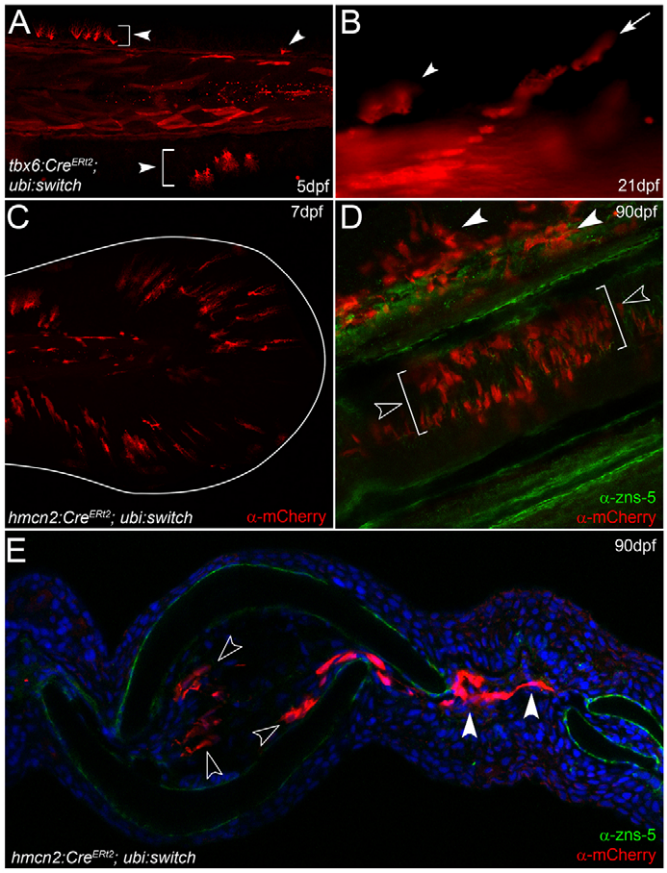

Fig. 6. Fin mesenchyme contributes to the adult fin fibroblasts. (**A**,**B**) *tbx6:Cre^{ERt2}; ubi:switch* transgenics treated with 4-hydroxytamoxifen and imaged at 5 dpf (A) and 21 dpf (B). Arrowheads indicate fin mesenchyme cells in the larval fin (A) and retained in juvenile fin (B). Chains of cells are seen invading at 21 dpf (arrow in B). (**C-E**) Images of *ubi:switch* transgenics injected with *hmcn2:Cre^{ERt2}* BAC transgene and treated with 4-hydroxytamoxifen from 3-4 dpf. (C) Tail region of 7-dpf larva shows mCherry in fin mesenchyme cells. The extent of the fin is outlined. (D,E) Adult fins immunostained for mCherry (red) and with zns-5 antibody (green) imaged in lateral whole-mount (D) or in transverse view following cryosectioning and counterstaining with DAPI (E). mCherry cells are in locations consistent with fibroblasts and are zns-5 negative. They reside within the fin rays (open arrowheads in D,E) or can be seen in the inter-ray region (white arrowheads in D,E).

against the existence of a neural crest stem cell in the trunk of fish that generates both neuronal/pigment and ectomesenchyme, which had previously been invoked as evidence for neural crest multipotency. It must be stressed that we have only interrogated the fates of trunk neural crest, which must be seen as distinct from questions of potency. Indeed, it has been reported that trunk neural crest cells are, under certain experimental conditions, able to generate bone, cartilage and dentine (Abzhanov et al., 2003; Lumsden, 1988; McGonnell and Graham, 2002). Our data argue that such permissive conditions do not exist in the tail/trunk of zebrafish. Conversely, we have demonstrated that the dermomyotome does respond to the fin environment, which promotes the immigration and differentiation of these cells into fibroblasts.

Little is known about the mechanisms controlling these events, and the zebrafish fin mesenchyme offers a tractable system with which to identify genetic and cellular systems controlling dermomyotome/fibroblast biology. Although our data demonstrate that these larval fin mesenchyme fibroblasts do not later contribute to the osteoblast lineage of the adult lepidotrichia (Lee et al., 2013), they do remain in the adult fins as fibroblasts. We suspect their function at this location is in modelling/repair of the ECM at these sites, in particular the actinotrichia of the distal adult lepidotrichia, mirroring their larval role. Indeed, during regeneration these cells have been observed to accumulate at the distal tip of the blastema (Nechiporuk and Keating, 2002; Poleo et al., 2001; Tu and Johnson, 2011), where actinotrichia form to guide regrowing lepidotrichia (Asharani et al., 2012; Durán et al., 2011). The regenerative plasticity of these fibroblasts within this distal blastema has been of interest to the fin regeneration field for a number of years; however, a number of recent reports indicate that fibroblasts do not normally regenerate other lineages after fin amputation (Knopf et al., 2011; Sousa et al., 2011; Stewart and Stankunas, 2012; Tu and Johnson, 2011). Recently, it has been shown that upon disruption of normal osteoblast regeneration, these fibroblasts may exhibit a degree of plasticity to compensate (Singh et al., 2012). Using our ability to label intra-ray fibroblasts, it will be interesting to determine the extent of plasticity exhibited by these cells during normal or perturbed fin regeneration.

We have now tested all three purported ectomesenchyme derivatives of trunk neural crest and found in all cases that they are mesoderm derived. Thus, the trunk neural crest of zebrafish is restricted, as is that of amniotes, to non-ectomesenchymal derivatives. The ability of trunk neural crest to generate ectomesenchyme was considered to be a feature of early vertebrates and central to the formation of the first mineralised skeleton of the vertebrate subphylum, the dermal armour of stem gnathostomes. The zebrafish fin mesenchyme and post-cranial exoskeleton were assumed to represent a relic of this early trunk neural crest ectomesenchyme (Smith et al., 1994). Our data cast doubt on this hypothesis and on the generation of ectomesenchymal derivatives from trunk neural crest in both fish and amniotes. By showing that the trunk exoskeleton and connective tissue cells of the fins are derived from mesodermal mesenchyme, our findings raise the possibility that the first mineralised skeleton of vertebrates was in fact of mesodermal origin.

Acknowledgements
We thank the V. Korzh lab. for supplying the ET37 and ET5 transgenic lines; the P. W. Ingham lab. for providing the *Tg(actc1b:Gal4)^{i269}* and *TgBAC(pax3a:EGFP)^{i150}* lines; the S. L. Amacher lab. for providing the *tbx6* promoter; the L. I. Zon lab. for the *ubi:switch* line; and the Zebrafish International Resource Center (University of Oregon, Eugene, OR 97403-5274, USA) for the zns-5 antibody.

Funding
This work was supported by the Biomedical Research Council of A*STAR (Agency for Science, Technology and Research), Singapore; the Zebrafish Initiative of the Vanderbilt University Academic Venture Capital Fund; and the National Institutes of Health National Institute of Dental and Craniofacial Research [grant R01 DE018477 to E.W.K.]. Deposited in PMC for release after 12 months.

Competing interests statement
The authors declare no competing financial interests.

Author contributions
R.T.H.L. and T.J.C. designed and performed experiments and wrote the paper. E.W.K. and J.P.T. provided reagents and edited the manuscript.

Supplementary material
Supplementary material available online at
http://dev.biologists.org/lookup/suppl/doi:10.1242/dev.093534/-/DC1

References

Abzhanov, A., Tzahor, E., Lassar, A. B. and Tabin, C. J. (2003). Dissimilar regulation of cell differentiation in mesencephalic (cranial) and sacral (trunk) neural crest cells in vitro. *Development* **130**, 4567-4579.

Asharani, P. V., Keupp, K., Semler, O., Wang, W., Li, Y., Thiele, H., Yigit, G., Pohl, E., Becker, J., Frommolt, P. et al. (2012). Attenuated BMP1 function compromises osteogenesis, leading to bone fragility in humans and zebrafish. *Am. J. Hum. Genet.* **90**, 661-674.

Baroffio, A., Dupin, E. and Le Douarin, N. M. (1991). Common precursors for neural and mesectodermal derivatives in the cephalic neural crest. *Development* **112**, 301-305.

Blentic, A., Tandon, P., Payton, S., Walshe, J., Carney, T., Kelsh, R. N., Mason, I. and Graham, A. (2008). The emergence of ectomesenchyme. *Dev. Dyn.* **237**, 592-601.

Breau, M. A., Pietri, T., Stemmler, M. P., Thiery, J. P. and Weston, J. A. (2008). A nonneural epithelial domain of embryonic cranial neural folds gives rise to ectomesenchyme. *Proc. Natl. Acad. Sci. USA* **105**, 7750-7755.

Carney, T. J., Dutton, K. A., Greenhill, E., Delfino-Machín, M., Dufourcq, P., Blader, P. and Kelsh, R. N. (2006). A direct role for Sox10 in specification of neural crest-derived sensory neurons. *Development* **133**, 4619-4630.

Carney, T. J., Feitosa, N. M., Sonntag, C., Slanchev, K., Kluger, J., Kiyozumi, D., Gebauer, J. M., Coffin Talbot, J., Kimmel, C. B., Sekiguchi, K. et al. (2010). Genetic analysis of fin development in zebrafish identifies furin and hemicentin1 as potential novel fraser syndrome disease genes. *PLoS Genet.* **6**, e1000907.

Chan, W. Y. and Tam, P. P. (1988). A morphological and experimental study of the mesencephalic neural crest cells in the mouse embryo using wheat germ agglutinin-gold conjugate as the cell marker. *Development* **102**, 427-442.

Chibon, P. (1967). Nuclear labelling by tritiated thymidine of neural crest derivatives in the amphibian Urodele Pleurodeles waltlii Michah. *J. Embryol. Exp. Morphol.* **18**, 343-358.

Collazo, A., Bronner-Fraser, M. and Fraser, S. E. (1993). Vital dye labelling of Xenopus laevis trunk neural crest reveals multipotency and novel pathways of migration. *Development* **118**, 363-376.

Davis, G. K., Jaramillo, C. A. and Patel, N. H. (2001). Pax group III genes and the evolution of insect pair-rule patterning. *Development* **128**, 3445-3458.

Detwiler, S. R. (1937). Observations upon the migration of neural crest cells, and upon the development of the spinal ganglia and vertebral arches in Amblystoma. *Am. J. Anat.* **61**, 63-94.

Dixon, G., Elks, P. M., Loynes, C. A., Whyte, M. K. and Renshaw, S. A. (2012). A method for the in vivo measurement of zebrafish tissue neutrophil lifespan. *ISRN Hematol.* **2012**, 915868.

Donoghue, P. C., Forey, P. L. and Aldridge, R. J. (2000). Conodont affinity and chordate phylogeny. *Biol. Rev. Camb. Philos. Soc.* **75**, 191-251.

Durán, I., Marí-Beffa, M., Santamaría, J. A., Becerra, J. and Santos-Ruiz, L. (2011). Actinotrichia collagens and their role in fin formation. *Dev. Biol.* **354**, 160-172.

DuShane, G. P. (1935). An experimental study of the origin of pigment cells in Amphibia. *J. Exp. Zool.* **72**, 1-31.

Dutton, J. R., Antonellis, A., Carney, T. J., Rodrigues, F. S., Pavan, W. J., Ward, A. and Kelsh, R. N. (2008). An evolutionarily conserved intronic region controls the spatiotemporal expression of the transcription factor Sox10. *BMC Dev. Biol.* **8**, 105.

Essex, L. J., Mayor, R. and Sargent, M. G. (1993). Expression of Xenopus snail in mesoderm and prospective neural fold ectoderm. *Dev. Dyn.* **198**, 108-122.

Feitosa, N. M., Zhang, J., Carney, T. J., Metzger, M., Korzh, V., Bloch, W. and Hammerschmidt, M. (2012). Hemicentin 2 and Fibulin 1 are required for epidermal-dermal junction formation and fin mesenchymal cell migration during zebrafish development. *Dev. Biol.* **369**, 235-248.

Gans, C. and Northcutt, R. G. (1983). Neural crest and the origin of vertebrates: a new head. *Science* **220**, 268-273.

Garriock, R. J. and Krieg, P. A. (2007). Wnt11-R signaling regulates a calcium sensitive EMT event essential for dorsal fin development of Xenopus. *Dev. Biol.* **304**, 127-140.

Gross, J. B. and Hanken, J. (2008). Review of fate-mapping studies of osteogenic cranial neural crest in vertebrates. *Dev. Biol.* **317**, 389-400.

Hall, B. K. and Hörstadius, S. (1988). *The Neural Crest. Including a Facsimile Reprint of The Neural Crest by Sven Hörsdtadius*. Oxford: Oxford University Press.

Harvey, S. A., Tümpel, S., Dubrulle, J., Schier, A. F. and Smith, J. C. (2010). no tail integrates two modes of mesoderm induction. *Development* **137**, 1127-1135.

Hatta, K., Tsujii, H. and Omura, T. (2006). Cell tracking using a photoconvertible fluorescent protein. *Nat. Protoc.* **1**, 960-967.

Holtfreter, J. (1935). Morphologische Beeinflussung von Urodelenektoderm bei xenoplastischer Transplantation. *Wilhelm Roux Arch. Entwickl. Mech. Org.* **133**, 367-426.

Horstadius, S. O. and Sellman, S. (1946). *Experimentelle Untersuchungen über die Determination des Knorpeligen Kopfskelletes bei Urodelen*. Stockholm: Almquist & Wiksell.

Inohaya, K., Takano, Y. and Kudo, A. (2007). The teleost intervertebral region acts as a growth center of the centrum: in vivo visualization of osteoblasts and their progenitors in transgenic fish. *Dev. Dyn.* **236**, 3031-3046.

Johnston, M. C. (1966). A radioautographic study of the migration and fate of cranial neural crest cells in the chick embryo. *Anat. Rec.* **156**, 143-155.

Kimmel, C. B., Ballard, W. W., Kimmel, S. R., Ullmann, B. and Schilling, T. F. (1995). Stages of embryonic development of the zebrafish. *Dev. Dyn.* **203**, 253-310.

Knopf, F., Hammond, C., Chekuru, A., Kurth, T., Hans, S., Weber, C. W., Mahatma, G., Fisher, S., Brand, M., Schulte-Merker, S. et al. (2011). Bone regenerates via dedifferentiation of osteoblasts in the zebrafish fin. *Dev. Cell* **20**, 713-724.

Krotoski, D. M., Fraser, S. E. and Bronner-Fraser, M. (1988). Mapping of neural crest pathways in Xenopus laevis using inter- and intra-specific cell markers. *Dev. Biol.* **127**, 119-132.

Kwan, K. M., Fujimoto, E., Grabher, C., Mangum, B. D., Hardy, M. E., Campbell, D. S., Parant, J. M., Yost, H. J., Kanki, J. P. and Chien, C. B. (2007). The Tol2kit: a multisite gateway-based construction kit for Tol2 transposon transgenesis constructs. *Dev. Dyn.* **236**, 3088-3099.

Landacre, F. (1921). The fate of the neural crest in the head of the urodeles. *J. Comp. Neurol.* **33**, 1-43.

Le Douarin, N. M. (1982). *The Neural Crest*. Cambridge: Cambridge University Press.

Le Douarin, N. M. and Kalcheim, C. (1999). *The Neural Crest*. New York, NY: Cambridge University Press.

Le Lièvre, C. S. and Le Douarin, N. M. (1975). Mesenchymal derivatives of the neural crest: analysis of chimaeric quail and chick embryos. *J. Embryol. Exp. Morphol.* **34**, 125-154.

Lee, R. T. H., Thiery, J. P. and Carney, T. J. (2013). Dermal fin rays and scales derive from mesoderm, not neural crest. *Curr. Biol.* **23**, R336-R337.

Lumsden, A. G. (1988). Spatial organization of the epithelium and the role of neural crest cells in the initiation of the mammalian tooth germ. *Development* **103** Suppl, 155-169.

Maurya, A. K., Tan, H., Souren, M., Wang, X., Wittbrodt, J. and Ingham, P. W. (2011). Integration of Hedgehog and BMP signalling by the engrailed2a gene in the zebrafish myotome. *Development* **138**, 755-765.

McGonnell, I. M. and Graham, A. (2002). Trunk neural crest has skeletogenic potential. *Curr. Biol.* **12**, 767-771.

Mongera, A. and Nüsslein-Volhard, C. (2013). Scales from fish arise from mesoderm. *Curr. Biol.* **23**, R338-R339.

Mosimann, C., Kaufman, C. K., Li, P., Pugach, E. K., Tamplin, O. J. and Zon, L. I. (2011). Ubiquitous transgene expression and Cre-based recombination driven by the ubiquitin promoter in zebrafish. *Development* **138**, 169-177.

Nechiporuk, A. and Keating, M. T. (2002). A proliferation gradient between proximal and msxb-expressing distal blastema directs zebrafish fin regeneration. *Development* **129**, 2607-2617.

Osumi-Yamashita, N., Ninomiya, Y., Doi, H. and Eto, K. (1994). The contribution of both forebrain and midbrain crest cells to the mesenchyme in the frontonasal mass of mouse embryos. *Dev. Biol.* **164**, 409-419.

Parinov, S., Kondrichin, I., Korzh, V. and Emelyanov, A. (2004). Tol2 transposon-mediated enhancer trap to identify developmentally regulated zebrafish genes in vivo. *Dev. Dyn.* **231**, 449-459.

Platt, J. B. (1893). Ectodermic origin of the cartilage of the head. *Anat. Anz.* **8**, 506-509.

Pohl, B. S. and Knöchel, W. (2001). Overexpression of the transcriptional repressor FoxD3 prevents neural crest formation in Xenopus embryos. *Mech. Dev.* **103**, 93-106.

Poleo, G., Brown, C. W., Laforest, L. and Akimenko, M. A. (2001). Cell proliferation and movement during early fin regeneration in zebrafish. *Dev. Dyn.* **221**, 380-390.

Raible, D. W. and Eisen, J. S. (1994). Restriction of neural crest cell fate in the trunk of the embryonic zebrafish. *Development* **120**, 495-503.

Raven, C. P. (1932). Zur entwicklung der ganglienleiste. I. Die kinematik der ganglienleistenentwicklung bei den urodelen. *Wilhelm Roux Arch. Entwickl. Mech. Org.* **125**, 210-292.

Raven, C. (1936). Zur Entwicklung der Ganglienleiste y. Über die Differenzierung des Rumpfganglienleistenmaterials. *Wilhelm Roux Arch. Entwickl. Mech. Org.* **134**, 122-146.

Schilling, T. F. and Kimmel, C. B. (1994). Segment and cell type lineage restrictions during pharyngeal arch development in the zebrafish embryo. *Development* **120**, 483-494.

Seger, C., Hargrave, M., Wang, X., Chai, R. J., Elworthy, S. and Ingham, P. W. (2011). Analysis of Pax7 expressing myogenic cells in zebrafish muscle development, injury, and models of disease. *Dev. Dyn.* **240**, 2440-2451.

Shimada, A., Kawanishi, T., Kaneko, T., Yoshihara, H., Yano, T., Inohaya, K., Kinoshita, M., Kamei, Y., Tamura, K. and Takeda, H. (2013). Trunk exoskeleton in teleosts is mesodermal in origin. *Nat. Commun.* **4**, 1639.

Singh, S. P., Holdway, J. E. and Poss, K. D. (2012). Regeneration of amputated zebrafish fin rays from de novo osteoblasts. *Dev. Cell* **22**, 879-886.

Sire, J. Y. and Akimenko, M. A. (2004). Scale development in fish: a review, with description of sonic hedgehog (shh) expression in the zebrafish (Danio rerio). *Int. J. Dev. Biol.* **48**, 233-247.
Sire, J. Y., Donoghue, P. C. and Vickaryous, M. K. (2009). Origin and evolution of the integumentary skeleton in non-tetrapod vertebrates. *J. Anat.* **214**, 409-440.
Smith, M. M. and Hall, B. K. (1990). Development and evolutionary origins of vertebrate skeletogenic and odontogenic tissues. *Biol. Rev. Camb. Philos. Soc.* **65**, 277-373.
Smith, M., Hickman, A., Amanze, D., Lumsden, A. and Thorogood, P. (1994). Trunk neural crest origin of caudal fin mesenchyme in the zebrafish Brachydanio rerio. *Proc. Biol. Sci.* **256**, 137-145.
Sobkow, L., Epperlein, H.-H., Herklotz, S., Straube, W. L. and Tanaka, E. M. (2006). A germline GFP transgenic axolotl and its use to track cell fate: dual origin of the fin mesenchyme during development and the fate of blood cells during regeneration. *Dev. Biol.* **290**, 386-397.
Sousa, S., Afonso, N., Bensimon-Brito, A., Fonseca, M., Simões, M., Leon, J., Roehl, H., Cancela, M. L. and Jacinto, A. (2011). Differentiated skeletal cells contribute to blastema formation during zebrafish fin regeneration. *Development* **138**, 3897-3905.
Stewart, S. and Stankunas, K. (2012). Limited dedifferentiation provides replacement tissue during zebrafish fin regeneration. *Dev. Biol.* **365**, 339-349.
Stone, L. S. (1926). Further experiments on the extirpation and transplantation of mesectoderm in Amblystoma punctatum. *J. Exp. Zool.* **44**, 95-131.
Stone, L. S. (1929). Experiments showing the role of migrating neural crest (mesectoderm) in the formation of head skeleton and loose connective tissue in Rana palustris. *Wilhelm Roux Arch. Entwickl. Mech. Org.* **118**, 40-77.
Suster, M. L., Sumiyama, K. and Kawakami, K. (2009). Transposon-mediated BAC transgenesis in zebrafish and mice. *BMC Genomics* **10**, 477.
Szeto, D. P. and Kimelman, D. (2004). Combinatorial gene regulation by Bmp and Wnt in zebrafish posterior mesoderm formation. *Development* **131**, 3751-3760.
Thisse, C. and Thisse, B. (2008). High-resolution in situ hybridization to whole-mount zebrafish embryos. *Nat. Protoc.* **3**, 59-69.
Tu, S. and Johnson, S. L. (2011). Fate restriction in the growing and regenerating zebrafish fin. *Dev. Cell* **20**, 725-732.
Tucker, A. S. and Slack, J. M. W. (2004). Independent induction and formation of the dorsal and ventral fins in Xenopus laevis. *Dev. Dyn.* **230**, 461-467.
Turner, S., Burrow, C. J., Schultze, H.-P., Blieck, A., Reif, W.-E., Rexroad, C. B., Bultynck, P. and Nowlan, G. S. (2010). False teeth: conodont-vertebrate phylogenetic relationships revisited. *Geodiversitas* **32**, 545-594.
Wang, W. D., Melville, D. B., Montero-Balaguer, M., Hatzopoulos, A. K. and Knapik, E. W. (2011). Tfap2a and Foxd3 regulate early steps in the development of the neural crest progenitor population. *Dev. Biol.* **360**, 173-185.
Weston, J. A., Yoshida, H., Robinson, V., Nishikawa, S., Fraser, S. T. and Nishikawa, S. (2004). Neural crest and the origin of ectomesenchyme: neural fold heterogeneity suggests an alternative hypothesis. *Dev. Dyn.* **229**, 118-130.

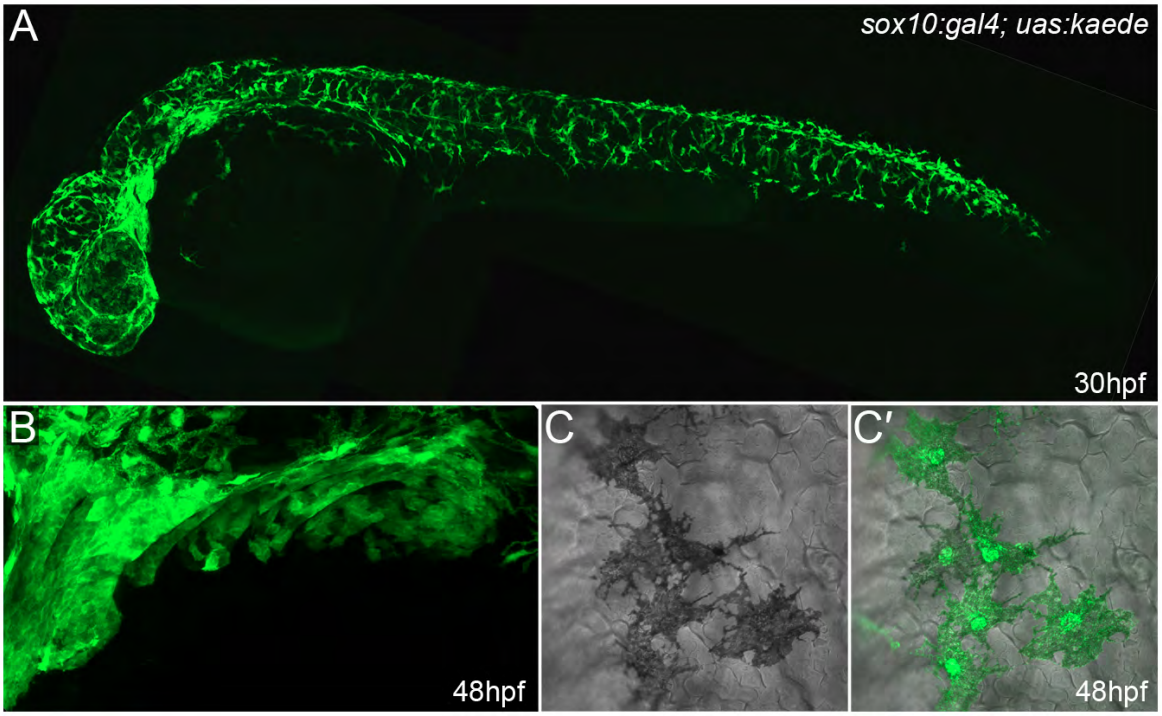

Fig. S1. Neural crest cells are well labelled in *sox10:gal4; uas:kaede* embryos. Lateral confocal images of 30-hpf (A,C,C′) and 48-hpf (B) *sox10:gal4; uas:kaede* transgenic embryos immunostained with an antibody detecting Kaede. (**A**) Broad and robust neural crest labelling along the entire axis can be seen at 30 hpf. (**B**) Lateral view of the branchial arches at 48 hpf showing extensive labelling of presumptive ectomesenchymal neural crest. (**C**,**C**′) Images showing DIC alone (C) or overlaid on a fluorescent image of Kaede expression demonstrates labelling of melanophores in *sox10:gal4; uas:kaede* transgenic embryos (C′). In this image, it can be seen that all five melanocytes express Kaede. Quantification of five 30-hpf *sox10:gal4; uas:kaede* transgenic embryos showed that at least 93.0% of melanophores are labelled by Kaede (a total of 545 melanophores was counted).

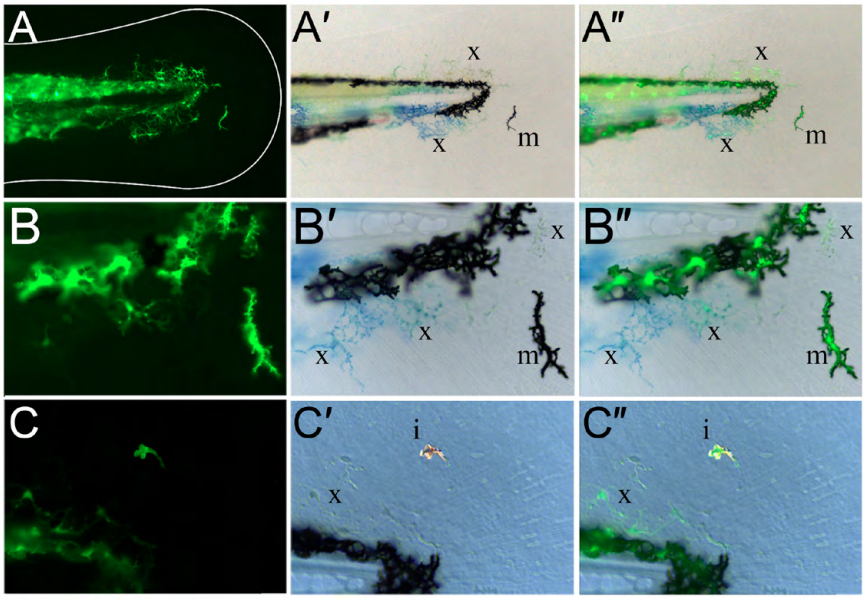

Fig. S2. Kaede-positive cells in the fin are chromatophores. (**A-C**″) Lateral views of the fin region of three 3-dpf *sox10:gal4; uas:kaede* transgenic embryos displaying Kaede green fluorescence (A,B,C) and brightfield views (A′,B′,C′). An overlay of the fluorescence image on the brightfield image is also shown (A″,B″,C″). At both low (A-A″) and high (B-C″) magnification, it can be observed that the Kaede-positive cells in the fin (A,B,C) correspond to black melanophores (m; A′,A″,B′,B″), xanthophores with characteristic yellow/blue colouration (x; A′,A″,B′,B″,C′,C″) or reflective iridophores (i; C′,C″).

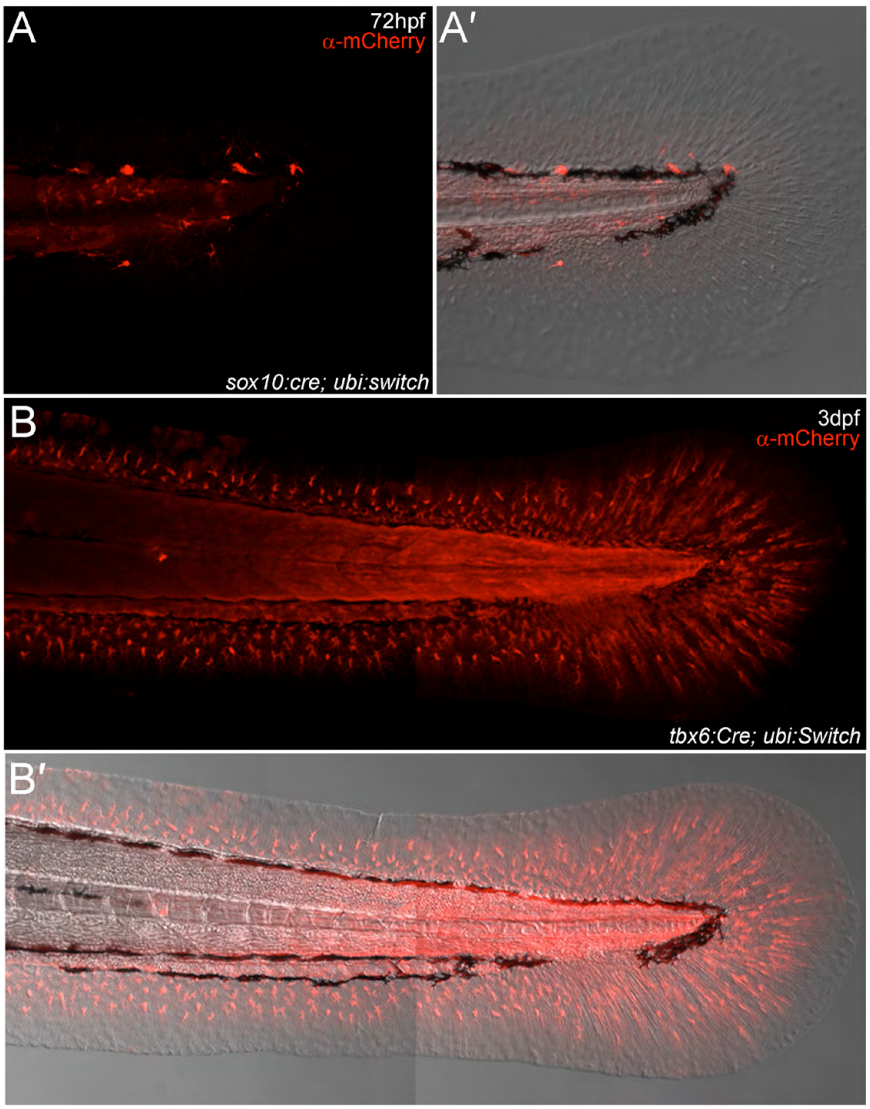

Fig. S3. Permanent lineage analysis confirms the origin of embryonic fin mesenchyme. (**A**,**A′**) Lateral confocal images of 72-hpf *sox10:Cre; ubi:switch* embryos fluorescently immunostained with an antibody detecting mCherry. Image of mCherry expression within the posterior trunk and fin (A) and also superimposed on a Nomarski view to show limited cells within the fin (A′). These embryos have neural crest lineages permanently labelled with mCherry, and show labelled cells within the trunk in locations and with morphology consistent with described neural crest derivatives. Fin mesenchyme is unlabelled. (**B**,**B′**) Lateral confocal images of 3-dpf *tbx6:Cre; ubi:switch* embryos fluorescently immunostained with an antibody detecting mCherry. (B) mCherry expression within the posterior trunk and fin with widespread expression visible in the fin mesenchyme and muscle of trunk. (B′) Fluorescent image superimposed on a Nomarski view outlining expression domains within the fin.

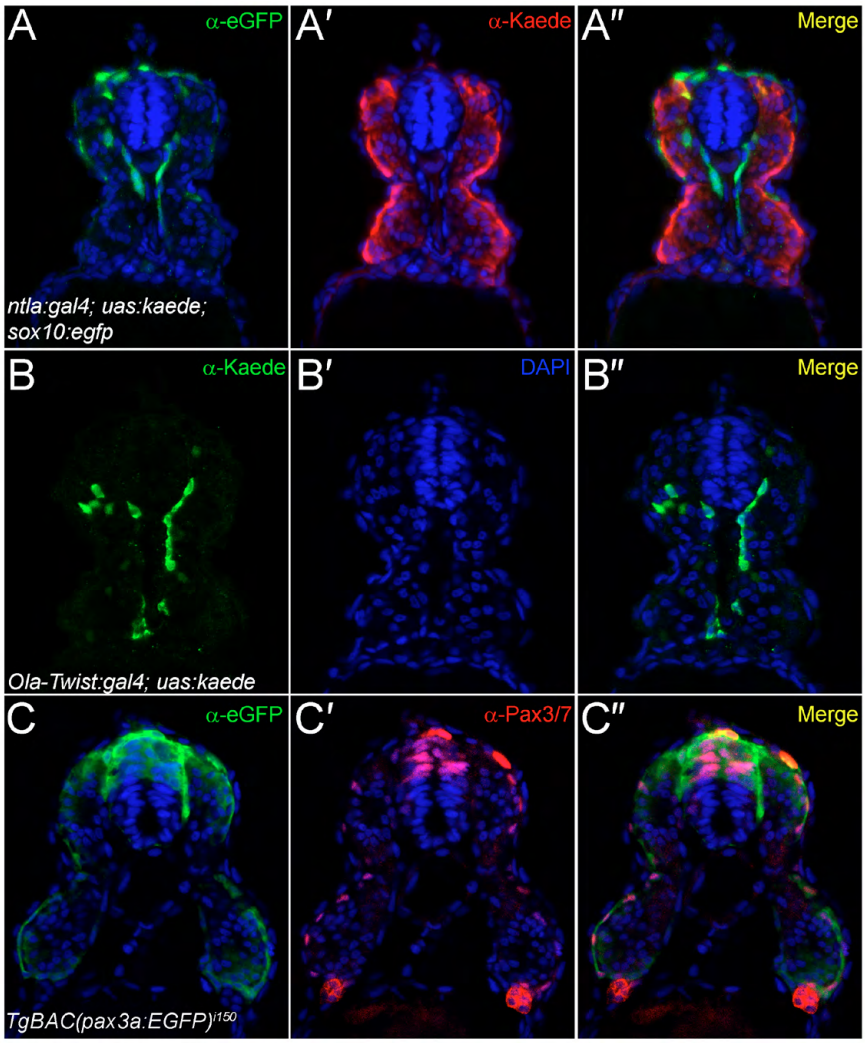

Fig. S4. Analysis of transgenic lines used to define the origin of fin mesenchyme. Transverse cryosections of the trunk region of the *ntla:gal4; uas:kaede* (A-A″), the *Ola-Twist:gal4; uas:kaede* (B-B″) and the *TgBAC(pax3a:EGFP)*^{i150} (C-C″) transgenic lines at 24 hpf, imaged by confocal microscopy following fluorescent immunostaining with antibodies against eGFP (A-A″,C-C″), Kaede (A-A″,B-B″) and Pax3/7 (C-C″). All sections were counterstained with DAPI (blue). (**A-A″**) To demonstrate exclusion of Kaede expression from neural crest, the *ntla:gal4; uas:kaede* line was crossed to the *sox10:egfp*^{ba2} line and immunostained for eGFP (A) and Kaede (A′). Restriction of Kaede to the mesoderm and exclusion from the neural crest can be seen in the superimposed image (A″). (**B-B″**) Expression of Kaede in the *Ola-Twist:gal4; uas:kaede* line is largely restricted to the sclerotomal compartment of the somites as seen by immunostaining for Kaede expression (B), which can be seen in a medial somitic location (B″) and far removed from the superficial dermomyotome domain. Occasional myotome expression can be observed in this line (B″). (**C-C″**) The *TgBAC(pax3a:EGFP)*^{i150} line faithfully recapitulates Pax3 expression in the dermomyotome as shown by comparing eGFP immunofluorescence (C) with Pax3/7 immunoreactivity (C′). By superimposition of the two confocal images, eGFP-positive dermomyotome cells at the somite surface have Pax3/7-positive nuclei, with strong eGFP and Pax3/7 colabelling in the dorsal neural tube and neural crest also apparent (C″).

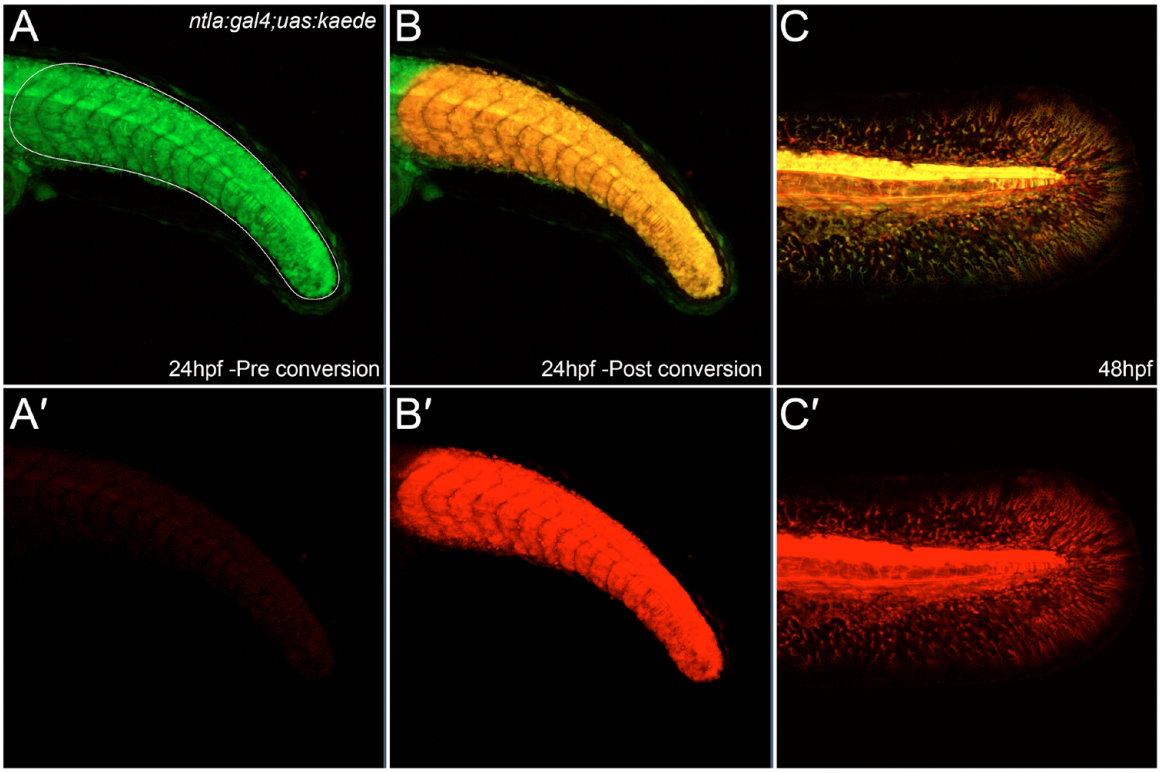

Fig. S5. Photoconversion of Kaede demonstrates that fin mesenchyme derives from earlier *ntla* mesoderm expression domains. (**A-C′**) The tail region of an *ntla:gal4; uas:kaede* transgenic embryo imaged at 24 hpf (A-B′) and again at 48 hpf (C,C′) both prior to (A,A′) and after (B-C′) Kaede photoconversion. Unconverted Kaede protein is shown in the green channel, which is overlaid with UV-photoconverted Kaede in the red channel (A,B,C). The red channel is additionally displayed alone for clarity (A′,B′,C′). The Kaede protein present at 48 hpf in the fin mesenchyme is photoconverted, demonstrating that it corresponds to perdurance of Kaede from the mesodermal expression domain at 24 hpf.

Movie 1. Ventral fin mesenchyme cells emerge from ventral somites. Confocal time-lapse movie of the tail region of an ET37 transgenic embryo imaged from 26 hpf for ~20 hours at 10-minute intervals. A fin mesenchyme cell is highlighted (arrow) leaving the ventral somite and taking up location in the ventral fin.

Movie 2. Dorsal fin mesenchyme cells emerge from dorsal somites. Confocal time-lapse movie of the tail region of an ET37 transgenic embryo imaged from 29 hpf for ~18 hours and 20 minutes at 8-minute intervals. A fin mesenchyme cell is highlighted (arrow) leaving the dorsal somite and taking up location in the dorsal fin.

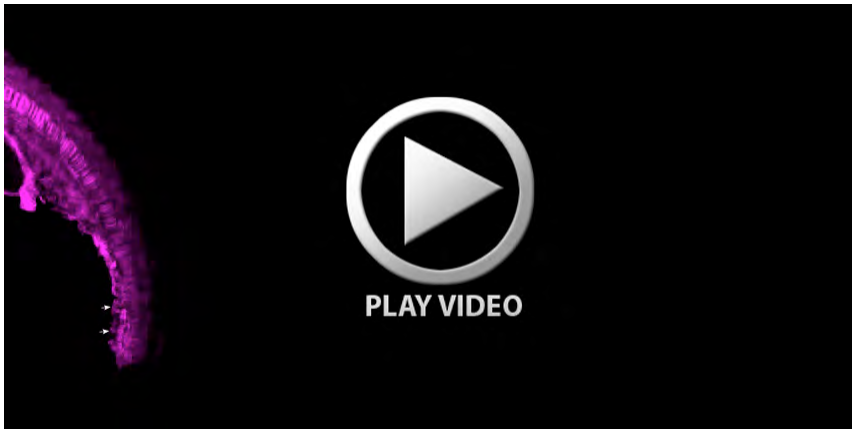

Movie 3. Fin mesenchyme emerges from an *ntla:lyn-tdtomato*-expressing somitic domain. Confocal time-lapse movie of the tail region of an *ntla:lyn-tdtomato* ET37 transgenic embryo, imaged from 22 hpf for ~12 hours at 8-minute intervals. The ET37 eGFP signal is shown in green, with membrane-tethered tdTomato driven by the *ntla* promoter in magenta. The first frame omits the GFP signals to highlight the epithelial nature of the tdTomato-expressing cells. Two cells, initially epithelial and expressing tdTomato, are indicated by arrows and followed out into the fin where they rapidly lose tdTomato expression and gain strong eGFP expression.

Movie 4. Fin mesenchyme derives from the *pax3a*-expressing dermomyotome. Confocal time-lapse movie of the tail region of a *TgBAC(pax3a:EGFP)*^{i150} transgenic embryo, imaged from 24 hpf for ~16 hours at 8-minute intervals. This line labels the neural crest, the dorsal neural tube and the dermomyotome, the latter being distinguishable from the former two as it has a less intense GFP signal. Fin mesenchyme cells can be tracked from the somite into the fins (two examples are indicated by arrows). Neural crest cells also invade the fins but show both increased intensity of GFP and migratory behaviour in comparison to the fin mesenchyme cells.